Supplementary Online Content

Rim JH, Lee S-T, Gee HY, et al. Accuracy of next-generation sequencing for molecular diagnosis in patients with infantile nystagmus syndrome. *JAMA Ophthalmol.* Published online November 16, 2017. doi:10.1001/jamaophthalmol.2017.4859

This supplementary material has been provided by the authors to give readers additional information about their work.

eTable 1. Target Genes Associated With Infantile Nystagmus Syndrome

Gene HGNC	Disease/Phenotype	OMIM Phenotype ID	Gene ID (OMIM#/GC)
ABCA4	Stargardt disease 1	248200	601691
ADAM9	Cone-rod dystrophy 9	612775	602713
ADAMTS18	Microcornea, chorioretinal atrophy, and telecanthus	615458	607512
AHI1	Joubert syndrome 3	608629	608894
AIPL1	Cone-rod dystrophy, Leber congenital amaurosis 4, RP juvenile	604393	604392
ALMS1	Alstrom syndrome	203800	606844
ARL13B	Joubert syndrome 8	612291	608922
ATF6	Achromatopsia 7	616517	605537
ATXN7	Spinocerebellar ataxia 7	164500	607640
BEST1	Bestrophinopathy, autosomal recessive	611809	607854
C10orf11	Albinism, oculocutaneous, type VII	615179	614537
C1QTNF5	Retinal degeneration, late-onset, autosomal dominant	605670	608752
C21orf2	Axial Spondylometaphyseal dysplasia	-	-
C5orf42	Joubert syndrome 17	614615	614571
C8orf37	Cone-rod dystrophy 16, RP 64	614500	614477
CABP4	Cone-rod synaptic disorder, congenital nonprogressive	610427	608965
CACNA1F	Night blindness, congenital stationary (incomplete), 2A	300071	300110
CACNA2D4	Retinal cone dystrophy 4	610478	608171
CAPN5	Vitreoretinopathy, neovascular inflammatory	193235	602537
CC2D2A	COACH syndrome	216360	612013
CDH3	Hypotrichosis, congenital, with juvenile macular dystrophy	601553	114021
CDHR1	Cone-rod dystrophy 15, RP 65	613660	609502
CEP290	Leber congenital amaurosis 10,	611755	610142
CEP41	Joubert syndrome 15	614464	610523
CERKL	RP 26	608380	608381
CFH	Macular degeneration, age-related, 4	610698	134370
CHM	Choroideremia	303100	300390
CNGA3	Achromatopsia 2	216900	600053
CNGB3	Achromatopsia 3	262300	605080
CNNM4	Jalili syndrome	217080	607850
COL11A1	Stickler syndrome, type II	604841	120280
COL11A2	Stickler syndrome, type III	184840	120290

COL2A1	Stickler syndrome, type 1	108300	120140
CRB1	Leber congenital amaurosis 8	613835	604210
CRX	Leber congenital amaurosis 7	613829	602225
CSPP1	Joubert syndrome 21	615636	611654
CYP27A1	Cerebrotendinous xanthomatosis	213700	606530
DRAM2	Cone-rod dystrophy 21	616502	613360
DTHD1	Leber congenital amaurosis	-	616979
EFEMP1	Doyne honeycomb degeneration of retina	126600	601548
ELOVL4	Stargardt disease 3	600110	605512
FRMD7	Nystagmus 1, congenital, X-linked	310700	300628
FSCN2	RP 30	607921	607643
FZD4	Exudative vitreoretinopathy 1	133780	604579
GDF6	Leber congenital amaurosis 17	615360	601147
GNAT2	Achromatopsia 4	613856	139340
GPR143	Ocular albinism, type I	300500	300808
GUCA1A	Cone-rod dystrophy 14	602093	600364
GUCA1B	RP 48	613827	602275
GUCY2D	Leber congenital amaurosis 1	204000	600179
HMCN1	Macular degeneration, age-related, 1	603075	608548
IFT140	Short-rib thoracic dysplasia 9 with or without polydactyly	266920	614620
IMPDH1	Leber congenital amaurosis 11	613837	146690
IMPG1	Macular dystrophy, vitelliform, 4	616151	602870
INPP5E	Joubert syndrome 1	213300	613037
IQCB1	Senior-Loken syndrome 5	609254	609237
JAG1	Alagille syndrome 1	118450	601920
KCNJ13	Leber congenital amaurosis 16	614186	603208
KCNV2	Retinal cone dystrophy 3B	610356	607604
KIF7	Joubert syndrome 12	200990	611254
LCA5	Leber congenital amaurosis 5	604537	611408
LRAT	Leber congenital amaurosis 14	613341	604863
MFN2	Charcot-Marie-Tooth disease, axonal, type 2A2A	609260	608507
NDP	Norrie disease	310600	300658
NMNAT1	Leber congenital amaurosis 9	608553	608700
NPHP1	Senior-Loken syndrome-1	266900	607100
OCA2	Albinism, oculocutaneous type II	203200	611409

OFD1	Joubert syndrome 10	300804	300170
OPA1	Optic atrophy 1	165500	605290
OPA3	Optic atrophy 3 with cataract	165300	606580
OTX2	Retinal dystrophy, early-onset, with or withour pituitary dysfunction	610125	600037
PANK2	Neurodegeneration with brain iron accumulation 1	234200	606157
PAX2	Papillorenal syndrome	120330	167409
PAX6	Foveal hypoplasia 1	136520	607108
PDE6C	Cone dystrophy 4	613093	600827
PDE6H	Achromatopsia 6	610024	601190
PITPNM3	Cone-rod dystrophy 5	600977	608921
POC1B	Cone-rod dystrophy 20	615973	614784
PRDM13	North Carolina macular dystrophy?	-	616741
PROM1	Cone-rod dystrophy 12	612657	604365
PRPH2	Leber congenital amaurosis 18	608133	179605
RAB28	Cone-rod dystrophy 18	615374	612994
RAX2	Cone-rod dystrophy 11	610381	610362
RD3	Leber congenital amaurosis 12	610612	180040
RDH12	Leber congenital amaurosis 13	612712	608830
RDH5	Fundus albitunctatus	136880	601617
RGS9	Bradyopsia	608415	604067
RGS9BP	Bradyopsia	608415	607814
RIMS1	Cone-rod dystrophy 7	603649	606629
RP1L1	Occult macular dystrophy	613587	608581
RPE65	Leber congenital amaurosis 2	204100	180069
RPGR	Cone-rod dystrophy, X-linked, 1	304020	312610
RPGRIP1	Leber congenital amaurosis 6	613826	605446
RPGRIP1L	Joubert syndrome 7	611560	610937
SEMA4A	Cone-rod dystrophy 10	610283	607292
SLC24A5	Albinism, oculocutaneous, type VI	113750	609802
SLC45A2	Albinism, oculocutaneous, type IV	606574	606202
SPATA7	Leber congenital amaurosis 3	604232	609868
TCTN3	Joubert syndrome 18	614815	613847
TIMP3	Sorby fundus dystrophy	136900	188826
TMEM126A	Optic atrophy 7	612989	612988

TMEM138	Joubert syndrome 16	614465	614459
TMEM216	Joubert syndrome 2	608091	613277
TMEM231	Joubert syndrome 20	614970	614949
TMEM237	Joubert syndrome 14	614424	614423
TMEM67	COACH syndrome	216360	609884
TTLL5	Cone-rod dystrophy 19	615860	612268
TULP1	Leber congenital amaurosis 15	613843	602280
TYR	Albinism, oculocutaneous, type IA	203100	606933
TYRP1	Albinism, oculocutaneous, type III	203290	115501
UNC119	?Cone-rod dystrophy	-	604011
WT1	Wilm's tumor, type I	194070	607102
ZNF423	Joubert syndrome 19	614844	604557

Table 1: Genes included in infantile nystagmus syndrome target enrichment. Listed are the genes included in the custom designed target enrichment along with the disease or phenotype associated with the gene according to Online Medelian Inheritance in Man (OMIM), OMIM phenotype identification number, and OMIM or Gene Cards gene identification number. Genes are named according HUGO Gene Nomenclature Committee (HUGO, http://www.genenames.org/) approved nomenclature.

eTable 2. Quality Control Matrices of Next-Generation Sequencing Results for all Patients In This Study

	Total reads (bam)	Mapped reads (bp, %)	Average depth	Median inserted fragment (bp)	On target (%)	% Covered (>X30)
Targeted panel	8,484,605	8,262,418 (97.7%)	990.4x	213.3	40.8	99.7%

eTable 3. The Clinical Features of Patients Who Had 2 Pathogenic Variants With No Segregation Analysis

Patient No.	Initial Clinical Impression	Molecular diagnosis	Diagnosis After revisit	Sex	Age (years)	Nystagmus	Refraction		BCVA	Fundus	Oculo Digital sign	ERG	Additional phenotype
29	LCA	*NMNAT 1*	LCA	F	1.75	Roving	+4.00	+5.00	NA	Atrophic macula	Y	extinguished	N
30	IIN	*RPGRIP 1*	LCA	M	28.3	HJ	-6.50	-6.50	0.05	Slight pale disc	N	extinguished	N
31	LCA	*CNGA3*	ACHM	M	9.5	HP	+6.00	+6.00	0.05	Grossly normal	N	Photopic: absent	N
32	ACHM	*CNGA3*	ACHM	F	1.2	HP	+2.75	+2.75	NA	Grossly normal	N	Photopic: absent	N

Abbreviations: ACHM, achromatopsia; BCVA, best-corrected visual acuity; ERG, electroretinography; F, female; HJ, horizontal jerk; HP, horizontal pendular; IIN, idiopathic infantile nystagmus; LCA, Leber congenital amaurosis; M, male; N, no; NA, not available; Y, yes

eTable 4. Pathogenic or Likely Pathogenic Variants in 4 Patients Who Had Compound Heterozygous Mutations With No Segregation Analysis

Patient No.	Initial diagnosis	Gene	Zygosity	Mutations	ExAC (MAF)	*In silico* prediction (FATHMM)	*Previous literatures*	Accession ID for transcript
29	LCA	*NMNAT1*	Compound heterozygous	c.196C>T: p.Arg66Trp c.709C>T: p.Arg237Cys	0.00013 0.000074	D (-6.60) D (-4.67)	Reference[1, 2] Reference[1, 2, 3]	NM_022787.3
30	IIN	*RPGRIP1*	Compound heterozygous	c.2079C>G: p.Tyr693Ter c.2009_2215+18del	none none	NA NA	Novel Novel	NM_020366.3
31	LCA	*CNGA3*	Compound Heterozygous	c.2T>A: p.Met1? c.1001C>T: p.Ser334Phe	none none	0.97342 D (-4.80)	Novel Reference[4]	NM_001298.2
32	ACHM	*CNGA3*	Compound heterozygous	c.829C>T: p.Arg277Cys c.1001C>T: p.Ser334Phe	0.00012 none	D (-5.78) D (-4.80)	Reference[5-10] Reference[4]	NM_001298.2

Abbreviations: ACHM, achromatopsia; D, damaging; ExAC, Exome Aggregation Consortium; FATHMM, Functional analysis through hidden Markov models; IIN, idiopathic infantile nystagmus; LCA, Leber congenital amaurosis; MAF, minor allele frequency

P30 was previously reported. (Reference 11)

References for eTable4.

1. Falk MJ, Zhang Q, Nakamaru-Ogiso E, et al. NMNAT1 mutations cause Leber congenital amaurosis. *Nat Genet.* 2012;44(9):1040-1045.

2. Sasaki Y, Margolin Z, Borgo B, Havranek JJ, Milbrandt J. Characterization of Leber Congenital Amaurosis-associated NMNAT1 Mutants. *J Biol Chem.* 2015;290(28):17228-17238.

3. Perrault I, Hanein S, Zanlonghi X, et al. Mutations in NMNAT1 cause Leber congenital amaurosis with early-onset severe macular and optic atrophy. *Nat Genet.* 2012;44(9):975-977.

4. Li S, Huang L, Xiao X, Jia X, Guo X, Zhang Q. Identification of CNGA3 mutations in 46 families: common cause of achromatopsia and cone-rod dystrophies in Chinese patients. *JAMA Ophthalmol.* 2014;132(9):1076-1083.

5. Wissinger B, Gamer D, Jagle H, et al. CNGA3 mutations in hereditary cone photoreceptor disorders. *Am J Hum Genet.* 2001;69(4):722-737.

6. Ding XQ, Fitzgerald JB, Quiambao AB, Harry CS, Malykhina AP. Molecular pathogenesis of achromatopsia associated with mutations in the cone cyclic nucleotide-gated channel CNGA3 subunit. *Adv Exp Med Biol.* 2010;664:245-253.

7. Huang L, Xiao X, Li S, et al. Molecular genetics of cone-rod dystrophy in Chinese patients: New data from 61 probands and mutation overview of 163 probands. *Exp Eye Res.* 2016;146:252-258.

8. Lam K, Guo H, Wilson GA, Kohl S, Wong F. Identification of variants in CNGA3 as cause for achromatopsia by exome sequencing of a single patient. *Arch Ophthalmol.* 2011;129(9):1212-1217.

9. Liu C, Varnum MD. Functional consequences of progressive cone dystrophy-associated mutations in the human cone photoreceptor cyclic nucleotide-gated channel CNGA3 subunit. *Am J Physiol Cell Physiol.* 2005;289(1):C187-198.

10. Lopez-Rodriguez A, Holmgren M. Restoration of proper trafficking to the cell surface for membrane proteins harboring cysteine mutations. *PLoS One.* 2012;7(10):e47693.

11. Han J, Rim JH, Hwang IS, et al. Diagnostic application of clinical exome sequencing in Leber congenital amaurosis. Mol Vis. 2017;20(23):649-659.

eTable 5. The Clinical Features of Patients With Infantile Nystagmus Syndrome With Only 1 Putative Pathogenic Variant or Unsolved Cases

Patient No.	Initial Diagnosis	Putative pathogenic variant	Sex	Age[a] (years)	Nystagmus	Refraction		BCVA	Fundus	Oculo Digital sign	ERG	Additional phenotype
						RE	LE					
33	LCA	*NMNAT1* c.709C>T	M	1.9	HJ	+6.75	+5.00	NA	Atrophic macula	Y	extinguished	N
34	LCA	*RPGRIP1* c.3565_3517del	F	1.25	Roving	+6.25	+6.25	NA	Slight pale disc	N	extinguished	encephalomalacia
35	LCA	*CEP290* c.4661_4663delAAG	F	1.6	HP	+4.25	+4.25	NA	Grossly normal	N	extinguished	N
36	IIN	*None*	M	5.6	HP	+0.575	+0.575	0.05	Optic atrophy Abnormal arcade vessel	N	NA	N
37	IIN	*None*	F	8.8	HP	+2.00	+2.00	0.5	Grossly normal	N	NA	N
38	IIN	*None*	F	16.3	HP	-4.00	-4.00	0.2	Grossly normal	N	NA	N
39	LCA	*None*	M	40.1	HJ	0	0	0.02	Chorioretinal atrophy	N	extinguished	Congenital cataract
40	OA	*None*	M	19.4	HP	+1.75	+2.25	0.2	Absence of foveal reflex, mild depigmented retina	N	NA	N
41	IIN	*None*	M	18.9	HP	-6.75	-6.75	0.1	Pigmentary retinopathy around macular	N	extinguished	N
42	LCA	*None*	M	3.6	Roving	+9.00	+9.00	NA	Pigmentary changes with mottling RPE	N	extinguished	MRI: Molar tooth sign

43	PAX6	*None*	F	0.6	Roving	NA	NA	NA	Absence of foveal reflex	N	NA	N
44	LCA	*None*	M	3.6	Roving	+1.00	+1.00	NA	Pigmentary retinopathy Optic atrophy	N	extinguished	Cerebellar atrophy
45	LCA	*ACO2 c.250C>T*	M	2.8	Roving	-1.25	-2.25	NA	Optic atrophy Grayish fundus	N	extinguished	Cerebellar atrophy
46	IIN	*None*	M	19.4	HP	-5.50	-2.75	0.3	Grossly normal	N	NA	N
47	LCA	*None*	M	1	Rotary	+4.50	+4.50	NA	Atrophic macula	N	extinguished	Delayed development
48	IIN	*None*	F	31.9	HJ	-8.25	-7.00	0.5	Grossly normal	N	NA	N

Abbreviations: BCVA, best-corrected visual acuity; ERG, electroretinography; F, female; HJ, horizontal jerk; HP, horizontal pendular; IIN, idiopathic infantile nystagmus; LCA, Leber congenital amaurosis; LE, left eye; M, male; N, no; NA, not available; OA, ocular albinism; RE, right eye, RPE, retinal pigment epithelium; Y, yes

[a]Age represents ages at last visit.

All variants were heterozygous, and all genes descripted in this table were known to be inherited as autosomal recessive.

P33 and P34 were previously reported. (Reference 1)

References for eTable5.

1. Han J, Rim JH, Hwang IS, et al. Diagnostic application of clinical exome sequencing in Leber congenital amaurosis. Mol Vis. 2017;20(23):649-659.

eAppendix. Annotation, Interpretation of Variants, Phenotype Review, and Consensus Discussion

First (step 1), variants were filtered by their frequencies in population control databases, including Exome Aggregation Consortium (non-TCGA dataset; frequencies were calculated according to ethnic subgroups), ESP6500, 1000 Genomes Project, and Korean Reference Genome DataBase. To maximize the diagnostic yield, variants with a minor allele frequency greater than 5% in any of the population subgroups rather than conventional 1% criteria were classified as absolutely benign, whereas those that were absent from the general population were considered to have moderate evidence as pathogenic. Secondly (step 2), literature and database searches for previous reports and functional studies were performed using the RetNet database, the Alamut Visual software and Human Gene Mutation Database professional database. Pathogenic or benign evidence was scored when predictions of all *in silico* algorithms agreed. Finally, the last step involved genetic specialists or laboratory physicians presenting a preliminary report to the patient's attending physicians or pediatric ophthalmologists, which listed all possible pathogenic variants, likely pathogenic variants, and variants of unknown significance (VUSs). When pathogenic or likely pathogenic variants were consistent with the patient's phenotype based on in-depth review by ophthalmologists, final validation using other confirmatory assays and a parental study was planned if available. VUSs, especially missense variants, were prioritized according to population frequency, American College of Medical Genetics score, and the patient's ocular phenotype. A parental study was scheduled to detect de novo occurrence for the candidate pathogenic or likely pathogenic variants, and VUSs in all available trios.

Systematic approaches for variant classification

Variant classification followed a three-step approach. First, conventional bioinformatics analysis found 16 variants in 15 patients that were classified as likely pathogenic based on the nature of the mutation (mostly null variants) and frequencies in the normal populations. No variant could be classified as definitely pathogenic during the first step. In the second step, extensive literature reviews and database searches were conducted for the variant and other variants in the same amino acid position. When combined with *in silico* analysis, 13 additional variants could be classified as likely pathogenic mutations and 5 variants previously classified as likely pathogenic after the first step were re-classified as pathogenic mutations during the second step. Diagnostic yield, which was calculated as the proportion of solved patients with sufficient pathogenic or likely pathogenic mutations among the 48 patients, increased from 14.9% to 25.5% during the second step. The third step included genotype-phenotype correlations, consensus discussion among geneticists and clinicians, family study and segregation results, and additional confirmatory assays. Finally, 24 variants could be identified as likely pathogenic and 19 variants identified as pathogenic in a total of 32 patients. The final diagnostic yield reached 66.7%.

eFigure 1. Schematic Diagram of Next-Generation Sequencing Analysis Work Flow

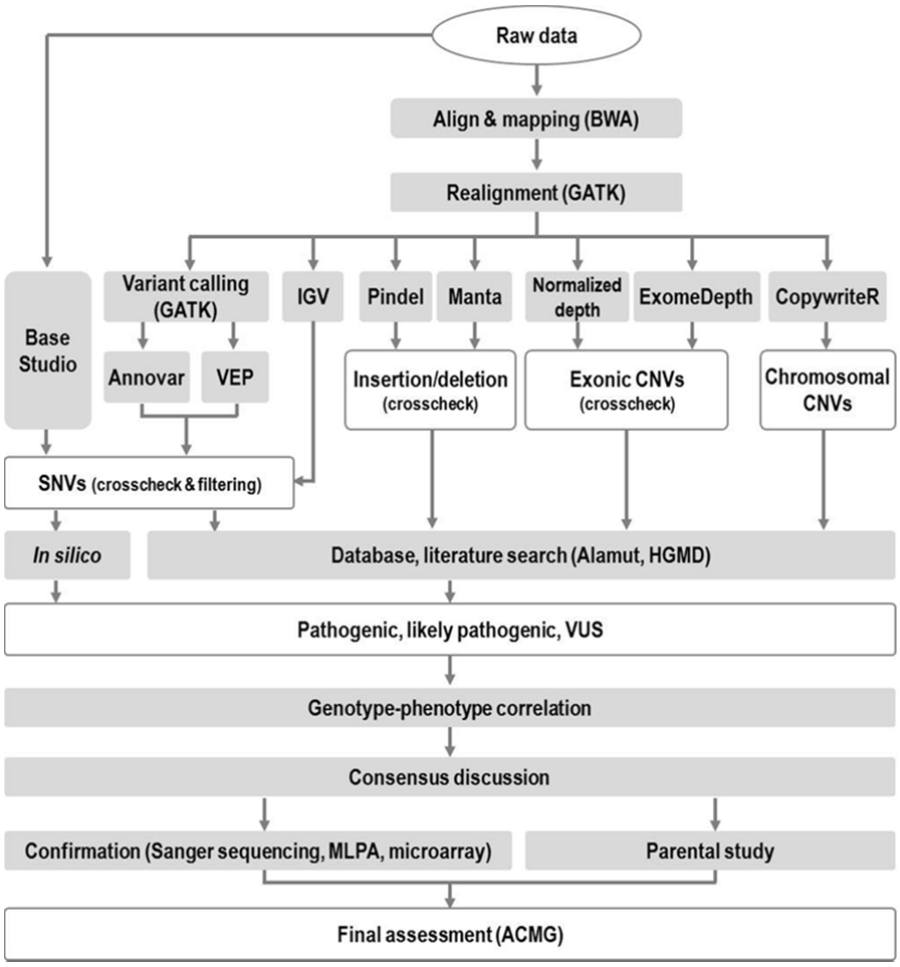

eFigure 2. Pedigree of 8 Patients Who Had Family History of Nystagmus

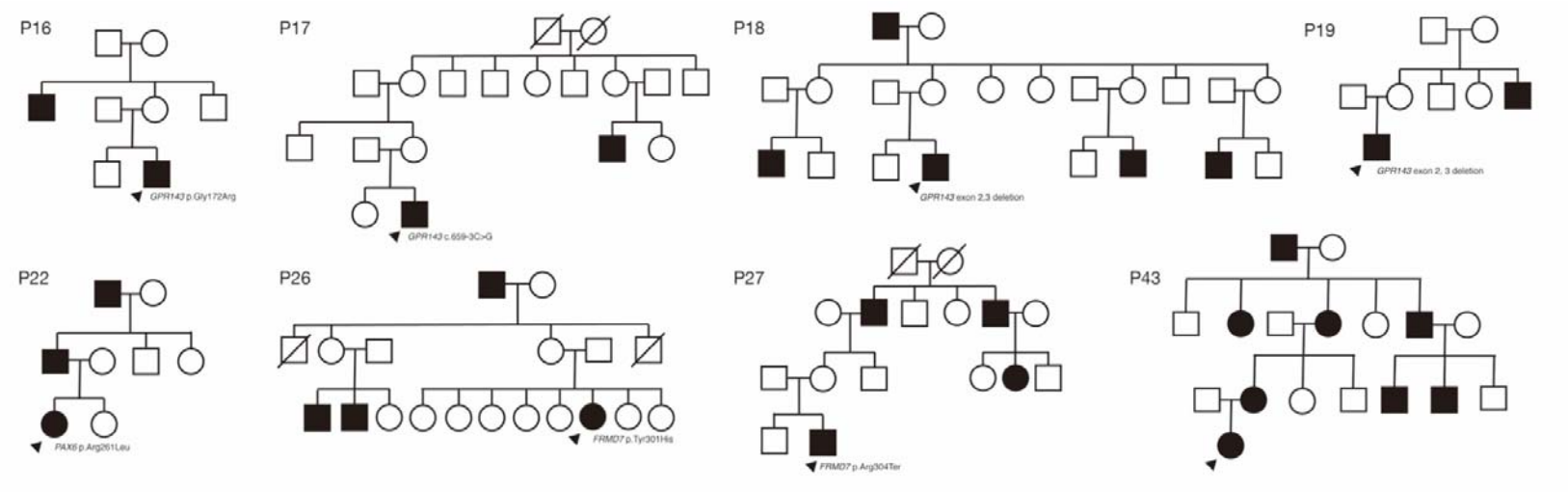

Targeted next-generation sequencing identified pathogenic or likely pathogenic variants in all patients except P43 with family history of aniridia.

eFigure 3. The Distribution of Age at the Time of Referral for Genetic Testing

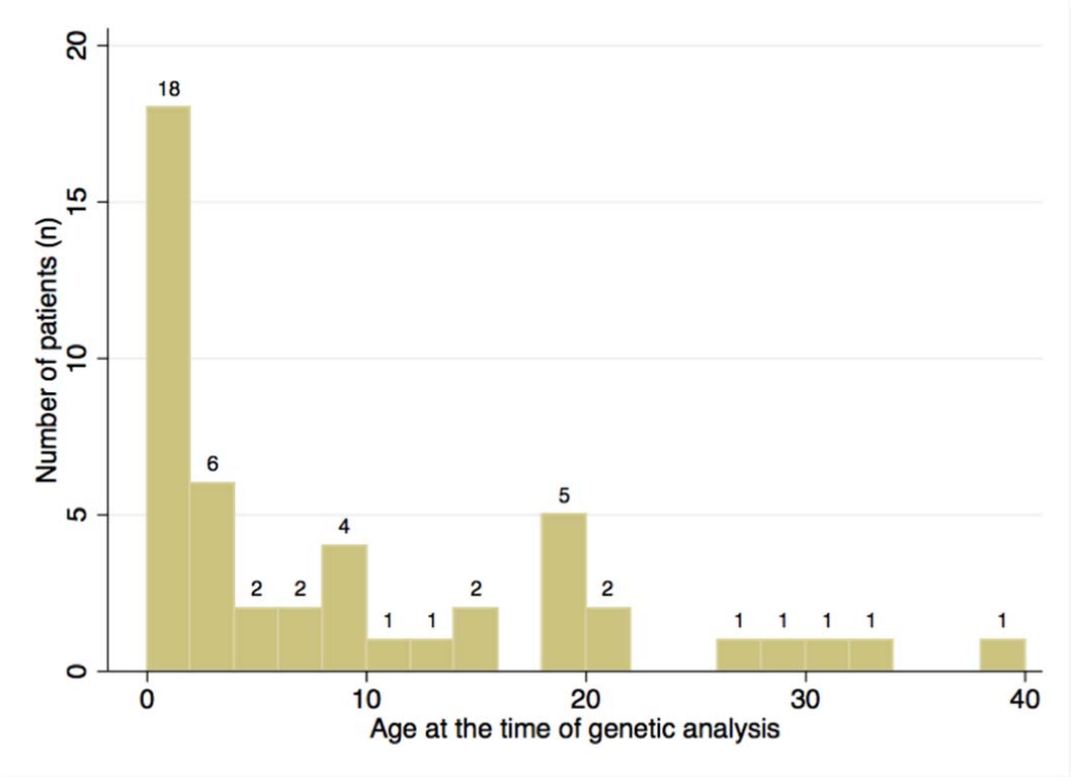

eFigure 4. Wide-Field Fundus Photograph and Optical Coherence Tomography in a Patient With *RPGRIP1* Mutations

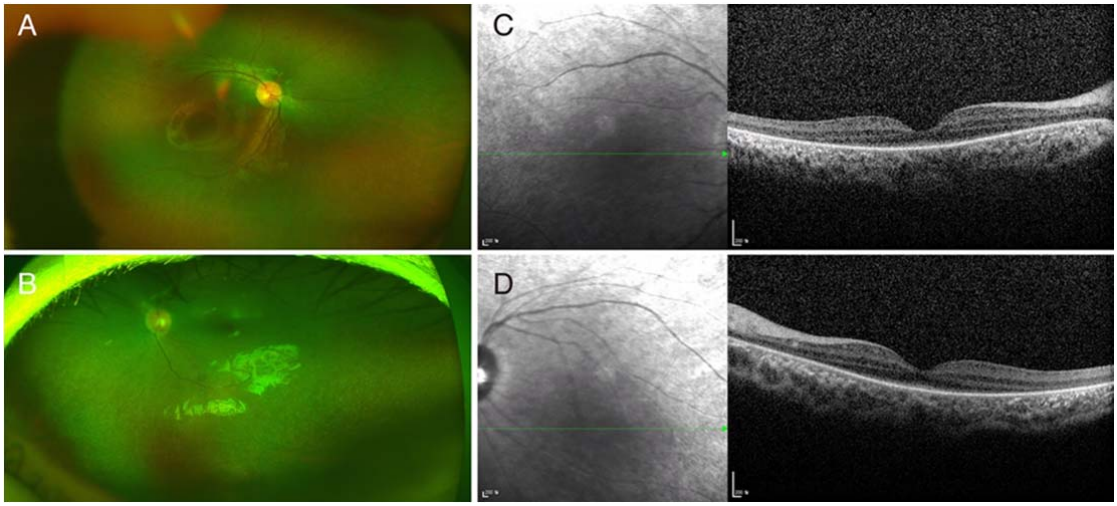

(P9) (A, B) Pigmentary retinopathy was seen in a patient with p.Arg768Ter and p.Arg1189GlyfsTer7 *RPGRIP1* mutations. (C, D) Diffuse loss of photoreceptor layers was noted in optical coherence tomography

eFigure 5. Fundus Photograph and Optical Coherence Tomography in a Patient With *CRB1* Mutations

(P13) 1 year old male came to our clinic for the evaluation of nystagmus. Patient exhibited 2Hz pendular nystagmus bilateral symmetric. He could fix and follow objects. Presumed clinical diagnosis of idiopathic infantile nystagmus was made on the basis of clinical findings. At the age of 4 years, parents reported that he had poked his eyes 1 years ago. Electroretinography showed extinguished ERG in both scotopic and photopic responses. Next-generation sequencing revealed compound heterozygous p.Ser403Ter/p.Arg526Ter *CRB1* mutations.(A, B) Granular pigmentary retinopathy was noted in both eyes. (C, D) Optical coherence tomography showed retinal thickening with loss of photoreceptor layers in both eyes.

eFigure 6. Fundus Photograph, Optical Coherence Tomography, Ultrasonography of the Kidney, and Abdominal Computed Tomography in a Patient With Senior-Loken Syndrome Caused by Homozygous p.Arg1178Glu *WDR19* Mutation

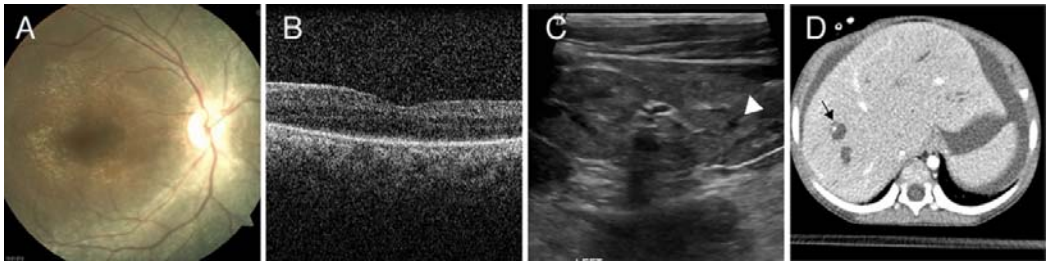

(P15) (A) Fundus photographs revealing pigmentary retinopathy. (B) Diffuse loss of photoreceptor layer was noted in optical coherence tomography. (C) Ultrasonography revealed increased parenchymal echogenicity and poor corticomedullary differentiation of both kidneys and cystic changes (arrowhead), which is suggestive of nephronophthisis. (D) Multifocal dilatation of intrahepatic bile ducts in both lobes of the liver (arrow), without significant common bile duct dilatation.

eFigure 7. Phenotypic Variability of 4 Patients With *GPR143* Mutations

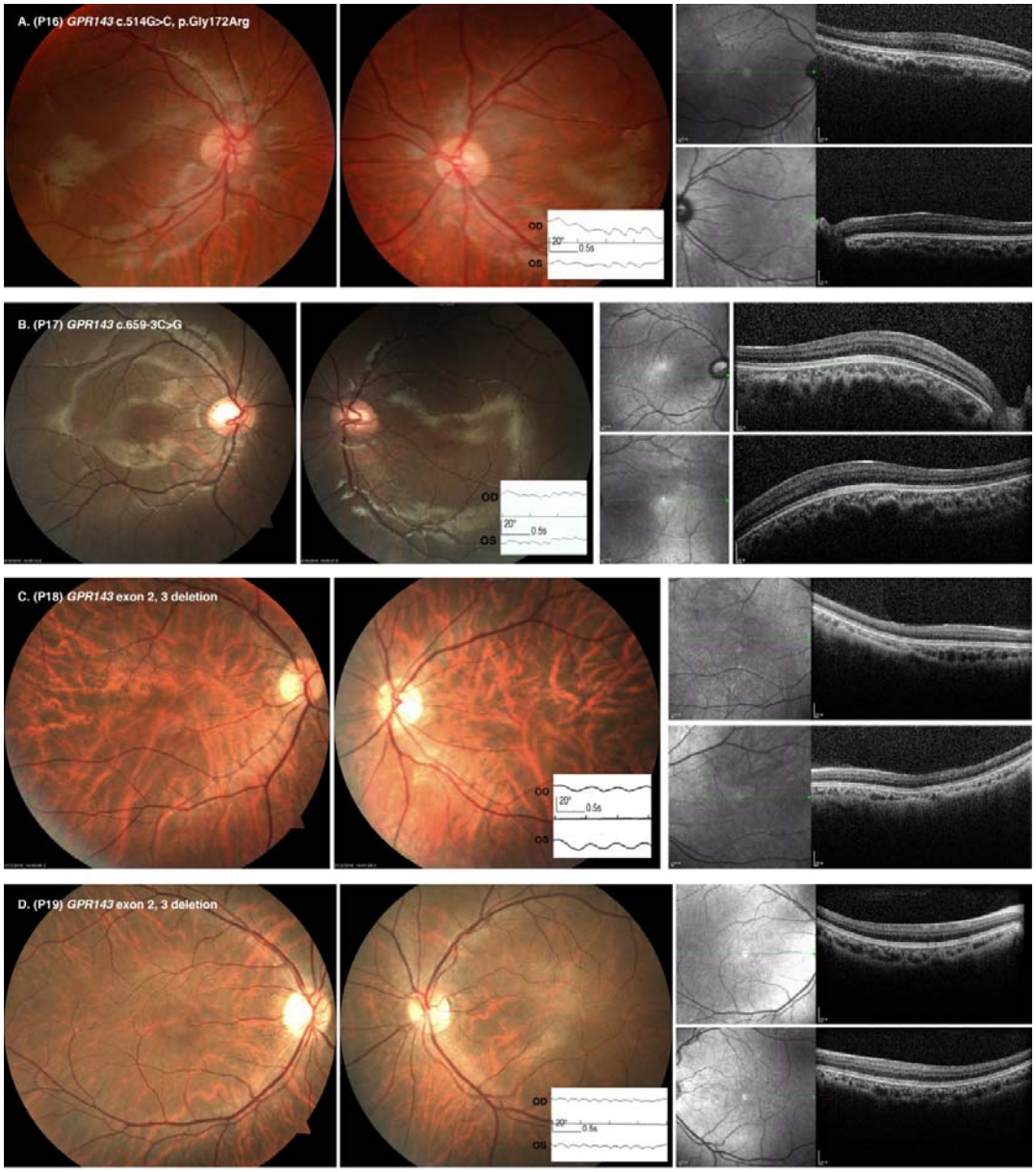

All patients had grade 4 foveal hypoplasia. (A) P16 had a missense mutation of *GPR143* c.514G→C, p.Gly172Arg. Depigmented fundi was noted, and 4 Hz pendular nystagmus was apparent. (B) P17 had a non-canonical splice site mutation of *GPR143* c.659-3C→G. *GPR143* c.659-3C→G mutation has not been previously reported in the literature; however, *in silico* predictions suggest that it introduces a strong 3′ splice acceptor site before the canonical 3′ splicing site of exon 5. Ocular pigmentation was normal in this patient. (C, D). *GPR143* exon 2, 3 deletion were found in P18 and P19. Depigmented retina was more severe in P18 than in P19. P18 had 2 Hz pendular nystagmus, but P19 had 4-5 Hz pseudocycloid nystagmus.

eFigure 8. *In silico* Prediction of Intronic Mutation Within *GPR143* Intron 5

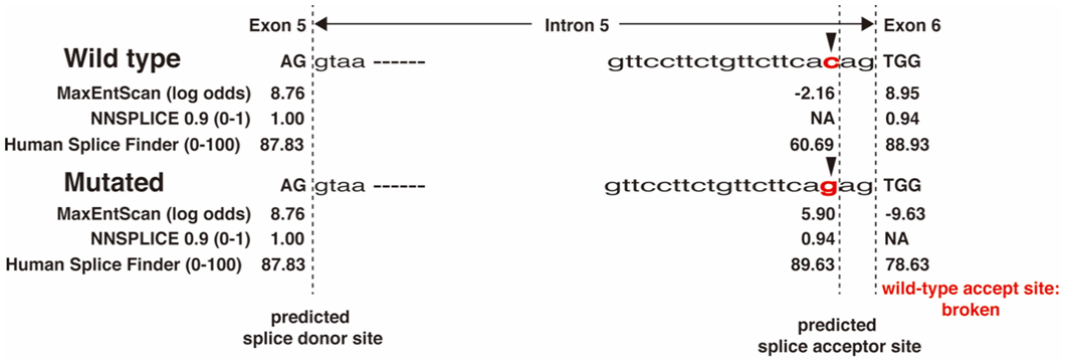

(P17) Predictions of splice sites in the wildtype and mutated *GPR143*. Diagram of the *GPR143* region comprising exons 5 and 6. Arrowheads indicate the mutated base. The scores calculated using MaxEntScan, NNSPLICE, and Human Splicing Finder v3.0 are depicted below each splice site. A higher score predicts a strong splice site. The values provided in parentheses indicate the score ranges in each algorithm. Note that scores of a potential cryptic splice donor site created by the mutation was almost the same levels as original splice acceptor sites, and mutation also caused wildtype acceptor site broken.

eFigure 9. Fundus Photographs and Optical Coherence Tomography in 4 Patients With *PAX6* Mutations

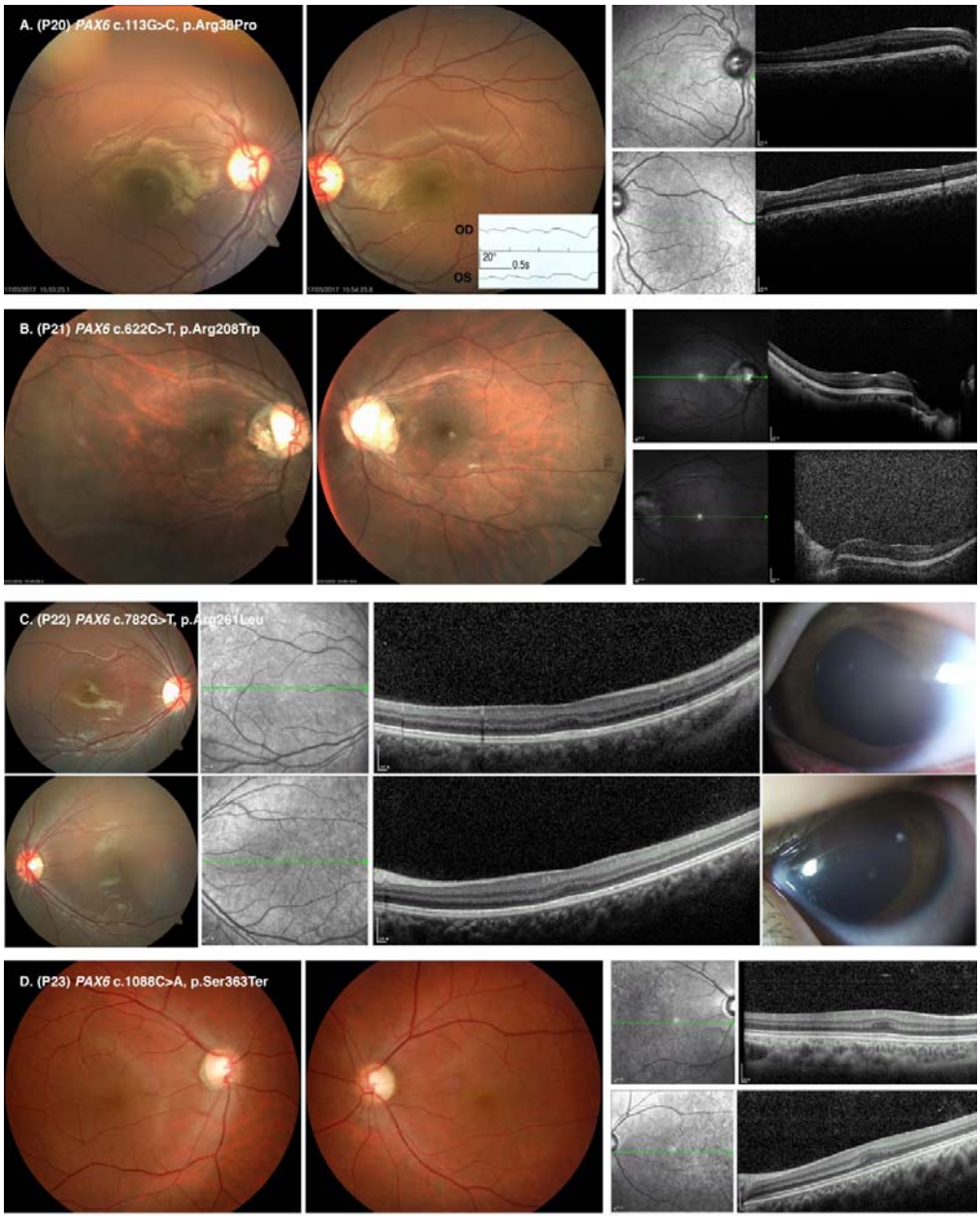

(A) p.Arg38Pro *PAX6* mutation was identified in P20. Optical coherence tomography (OCT) revealed grade 2 foveal hypoplasia. Posterior subcapsular cataract was noted in this patient. (B) 26-year-old male visited the clinic for genetic testing for nystagmus. He underwent cataract surgery due to presenile cataract at the age of 24 years. Iris structure was normal in this patient. Grade 1 foveal hypoplasia was noted in OCT. (C) 8-year-old girl had nystagmus and grade 3 foveal hypoplasia. p.Arg261Leu *PAX6* mutation was detected in targeted next-generation sequencing. (D) Novel nonsense p.Ser363Ter *PAX6* mutation was identified in P23. Horizontal pendular nystagmus was noted. This patient had grade 3 foveal hypoplasia and normal iris structure without presenile cataract.

eFigure 10. Fundus Photograph and Electroretinography in a Patient With *CACNA1F* Mutation

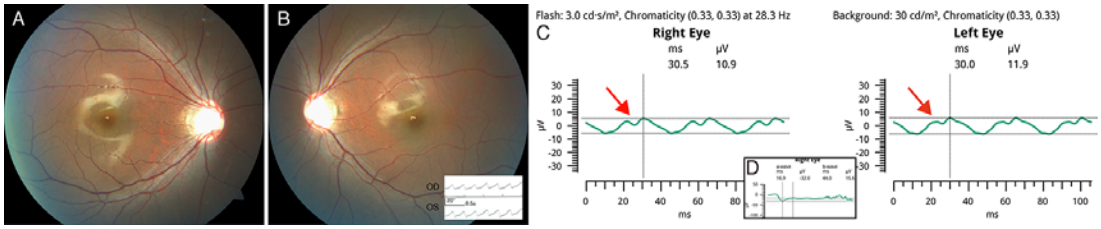

(P28) A 1.5 year-old boy came to our clinic for the evaluation nystagmus. Ocular motility examination showed 2Hz right-left alternating jerk nystagmus. (A, B) Fundus examination showed high cup disc ratio. Cycloplegic refraction showed mild myopia at the age of 1.5 years. At the age of 5 years, best corrective visual acuity was 20/100 in both eyes and myopia progressed to moderate myopia. Optical coherence tomography showed normal retinal lamellar structures at fovea. Targeted next-generation sequencing revealed a hemizygous c.342delC, p.Phe114SerfTer22 *CACNA1F* mutation. (C, D) Electroretinography (ERG) showed negative ERG in dark-adapted 3.0 ERG and “double peak” sign in light-adapted 3.0 flicker.